Hydraulic performance of stepped spillways with reverse step barriers under skimming flow conditions: a three-dimensional numerical study

Dana Ghaderi [1], Hamzeh Ebrahimnezhadian [2], Mahdi Mollazadeh [1,*]

1. Department of Civil Engineering, University of Birjand, Birjand, Iran.
2. Department of hydraulic structures, Urmia, Iran.

***Corresponding Author:**
Mahdi Mollazadeh

Email: mollazadeh.mahdi@birjand.ac.ir
Received: 2026.04.30
Accepted: 2026.09.03
J. Hydraul. Struct., 13(1):71-87
DOI: 10.22055/jhs.2026.51891.1379

ABSTRACT

In recent years, the application of stepped spillways has increased owing to their high efficiency. Therefore, studies in this field have been of interest to researchers. Most of the studies have been focused on improving the ability of energy dissipation. In this research, a special configuration was presented named stepped spillway with reverse step barriers, and its energy dissipation capability was evaluated in comparison with conventional stepped spillways. The numerical model was validated against experimental results obtained from the physical model. OpenFOAM was used to develop five three-dimensional reverse step barrier configurations designed for skimming flow. The flow was simulated using the InterFoam solver with the RNG k–ε turbulence model. The findings reveal a substantial enhancement in energy dissipation toward the downstream section of the spillway. Also, among the different configurations, G2 geometry exhibited the highest energy dissipation rate. At a discharge of 0.09 m^3/s and a yc/h ratio of 1.45, the G2–G5 configurations achieved greater energy dissipation than the conventional stepped spillway, with increases of 64.1%, 26.4%, 41.5%, and 54.7% for G2, G3, G4, and G5, respectively. Finally, G2 geometry was proposed as the best-performing configuration in stepped spillways with reverse step barriers in terms of energy dissipation rate.

KEYWORDS

Stepped spillway, Computational fluid dynamics, OpenFOAM software, Energy dissipation, Reverse step barriers.

1. Introduction

The use of stepped spillways for flow management dates back to ancient times. According to the historical review by Chanson [1], one of the earliest documented examples of a stepped spillway is the Koufonisi Dam in Greece, which is estimated to have been constructed around 1000 BC. The development and widespread implementation of Roller-Compacted Concrete (RCC) technology in recent decades have led to renewed interest in stepped spillways, particularly because of their structural stability and effective energy dissipation capability. Meanwhile, advances in dam construction technology have made the construction of very large dams increasingly feasible. The high height of the dams causes the flow velocity to increase to a very high extent during the discharge and extraction of water from the dam and causes phenomena such as cavitation, erosion and scouring of the downstream bed. Therefore, an energy dissipation system is needed in the way of discharging the flow from the dams. Dams with a higher height require a more efficient energy dissipation system.

In recent years, scholars have focused on enhancing the efficiency of spillways and have undertaken extensive research in this domain. One notable area of investigation involves optimizing energy dissipation in stepped spillways to mitigate downstream flow velocity. Sorensen [2], Peyras et al. [3], and Rice et al. [4] examined the effect of flow regime, step geometry, and spillway slope on energy dissipation. Extensive laboratory investigations on the identification of flow type and energy dissipation in stepped spillways have been conducted by Chanson [5] and relationships to distinguish the flow type and quantify the energy dissipated in these spillways has also proposed. Felder and Chanson [6] investigated a stepped spillway inclined at 21.8°, with the analysis conducted for two step configurations measuring 5 and 10 cm in height. The two-phase flow characteristics in high-velocity conditions were investigated for flow passing over a stepped chute. The downstream energy dissipation associated with reverse slopes, step geometry, step-end edges, and surface roughness was examined by Felder et al. [7,8], Hamedi et al. [9], and Nohani [10]. Li and Zhang [11] conducted numerical simulations to investigate the hydraulic behavior of various pooled stepped spillway configurations, with particular attention to vortex formation mechanisms and the corresponding pressure and velocity distributions. Ma et al. [12] investigated numerically the energy dissipation in interval-pooled stepped spillways. Using the Omega vortex-intensity criterion, the study demonstrated that stepped spillways equipped with V-shaped and inverted V-shaped steps provide greater energy dissipation than conventional flat-step and continuous pool-type configurations. In addition, the average intensity of the vortex can determine the rate of energy dissipation to some extent.

Salmasi and Abraham [13] investigated the performance of stepped spillways as an effective hydraulic structure for flow energy dissipation. In their study, the effects of key design parameters, including step width, step height, spillway slope, and spillway height, on the hydraulic performance of the system were evaluated. Owing to the large number of design variables, the nonlinear nature of the objective function, and the associated design constraints, a genetic algorithm was employed to determine the optimal spillway dimensions. Their results demonstrated that increasing the number of steps enhanced energy dissipation, while the sensitivity analysis indicated that the relative energy dissipation decreased with increasing spillway slope. These findings highlighted the importance of optimal stepped-spillway design for improving the hydraulic efficiency of spillway structures. In another study, Salmasi and Abraham [14] conducted an experimental and numerical investigation of stepped spillways to evaluate their energy dissipation performance. Nine physical models with spillway slopes of 15°, 25°, and 45° and varying numbers of steps (5–50) were constructed to examine the effects of these parameters on energy dissipation. The experimental results revealed that the dimensionless parameters, namely the Froude number and ($q^2/(gH_{dam}^3)$), exerted the greatest influence on energy dissipation, whereas the spillway slope and the number of steps had a comparatively smaller effect on the overall energy dissipation rate. Nevertheless, for a constant discharge, increasing both the spillway slope and the number of steps resulted in greater energy dissipation

Salmasi and Abraham [15] numerically investigated the hydraulic behavior of skimming flow along the stepped spillway of the Zirdan Dam. The hydraulic performance of stepped and smooth spillways was assessed through numerical simulations based on the RNG k–ε turbulence formulation and the multiphase

mixture approach. The numerical model was validated against field measurements. The findings demonstrated that the steps significantly reduced the boundary-layer development length and promoted earlier flow aeration. Moreover, the cavitation index along the stepped spillway remained consistently above the critical threshold, indicating a negligible risk of cavitation damage. In contrast, the smooth spillway exhibited the potential for cavitation (negative pressure) beginning approximately 56 m downstream of the spillway crest. In another experimental study, Salmasi *et al.* [16] evaluated the influence of various hydraulic parameters on flow energy dissipation in gabion stepped spillways. Particular attention was given to the hydraulic performance of rectangular and inclined end sills. The results indicated that the effectiveness of end sills was considerably greater in gabion spillways with milder slopes than in those with steeper slopes. Furthermore, rectangular end sills produced approximately 3–4% higher energy dissipation than inclined end sills. The study also demonstrated that gabion material with a median particle diameter (d_{50}) of 10mm provided the highest energy dissipation efficiency. These findings emphasize the importance of end-sill geometry in the hydraulic performance of gabion stepped spillways and provide practical guidance for improving energy dissipation in similar hydraulic structures.

Ghaderi et al. [17] conducted a combined numerical and experimental investigation to evaluate the influence of labyrinth configurations with trapezoidal and rectangular crest geometries on the energy dissipation rate of stepped spillways. Using an OpenFOAM-based numerical model with the InterFoam solver, the hydraulic performance of these configurations was compared with that of a conventional stepped spillway under skimming flow conditions. The results demonstrated that modifying the labyrinth crest geometry to trapezoidal and rectangular forms significantly enhanced the energy dissipation performance. For a flow condition characterized by (y_c/h=1.45), the trapezoidal and rectangular configurations achieved 34.7% and 21.1% greater energy dissipation, respectively, relative to the conventional stepped spillway. The pressure field and turbulent kinetic energy were also examined, showing that the trapezoidal configuration produced higher turbulent kinetic energy, whereas the rectangular configuration resulted in more pronounced negative pressures over the upper half of the vertical step face. These findings emphasize the need to account for structural performance and potential cavitation when designing labyrinth stepped spillways. In a subsequent study, Ghaderi et al. [18] employed an OpenFOAM-based numerical model, validated against experimental data, to investigate the hydraulic characteristics, energy dissipation rate, and residual energy downstream of stepped spillways incorporating circular labyrinth crest configurations. Their results showed that combining a stepped spillway with circular labyrinth crest geometries enhanced energy dissipation compared with a conventional stepped spillway. At a constant discharge corresponding to (y_c/h=1.68), the two-cycle, three-cycle, and four-cycle arrangements yielded energy dissipation enhancements of 4.7%, 28.0%, and 18.3%, respectively. Of all the configurations examined, the three-cycle arrangement provided the greatest energy dissipation and exhibited less severe negative pressures over the upper half of the vertical step face, demonstrating its enhanced hydraulic and structural performance.

A review of the existing literature indicates that stepped spillways have been extensively investigated over the past decades from various perspectives,

including step geometry, surface roughness, localized cavities, spillway curvature, and optimization techniques. However, to the best of the authors' knowledge, previous studies have primarily focused on conventional geometric modifications, while stepped spillways incorporating reverse step barriers as a distinct hydraulic configuration have not yet been investigated. Therefore, the present study introduces and evaluates, for the first time, several novel configurations incorporating reverse step barriers with different arrangements. Their hydraulic performance is assessed in terms of energy dissipation and compared with that of a conventional stepped spillway. The findings of this study are expected to contribute to the advancement of current knowledge on stepped spillway design and to identify more effective configurations for enhancing flow energy dissipation.

2. Materials and methods

2.1. Theoretical Relations of Flow Regime Detection

Several experimental and theoretical relationships have been introduced in the literature to determine the governing flow regime in stepped spillways. The flow regime can be effectively characterized based on the discharge rate and the geometric characteristics of the spillway steps. Various researchers, including Rajaratnam [19], Peyars et al. [3], and Chanson [20] have conducted studies that demonstrate the dependence of flow type on the normalized critical depth (y_c/h) and the dimensionless coordinate of the step (h/l). Here, yc represents the critical flow depth, while h and l represent the step height and length, respectively. Accordingly, the following experimental relationships are presented based on the conditions in which the skimming flow regime is established, as proposed by various researchers.

$$\frac{y_c}{h} \geq 0.8 \qquad 0.4 \leq \frac{h}{l} \leq 0.9 \qquad \text{Rajaratnam [19]} \qquad (1)$$

$$\frac{y_c}{h} \geq 1.01 - 0.37\left(\frac{h}{l}\right) \qquad \text{Peyars et al.[3]} \qquad (2)$$

$$\frac{y_c}{h} \geq 1.05 - 0.465\left(\frac{h}{l}\right) \qquad 0.2 \leq \frac{h}{l} \leq 1.25 \qquad \text{Chanson [20]} \qquad (3)$$

Based on Equations (1)–(3) and the information given in Table 1, it can be concluded that the simulated flow regime in this study is classified as skimming flow.

Table 1: Flow parameters and associated flow patterns of the investigated stepped spillway in this study.

Discharge(m^3/s)	$y_c=(q^2/g)^{(1/3)}$	Step height,h (m)	Step width, l(m)	h/l	y_c/h	Flow regime
0.09	0.145	0.1	0.2	0.5	1.45	skimming

2.2. Dimensional Analysis

According to the findings of previous researchers, the parameters influencing flow over stepped spillways include dynamic viscosity (μ), density (ρ), gravitational acceleration (g), flow depth (y), flow velocity (V), step height (h), step width (l), number of steps (N_0), spillway width (W), and spillway height ($H_{spillway}$). Other parameters of spillways with reverse step barriers are not presented because they are the same in all models. When the width (W) is significantly larger than the flow depth (y), the dissipation of energy in stepped spillways is influenced by various factors such as the number of steps (N_0), step

height (h), step width (l), and flow rate (Q). Therefore, various parameters in the reverse step slope spillways are related in the form of equation (4). By applying Buckingham's π theorem and using density (ρ), flow depth (y), and flow velocity (V) as repeating parameters, the relative energy dissipation can be expressed as a function of the following dimensionless parameters.

$$\frac{\Delta H}{H_0} = f\left(\frac{y_c}{h}, \frac{y_c}{l}, \frac{H_{spillway}}{W}, R_e, Fr, N_0\right) \qquad (4)$$

If it is assumed that in open channels, inertial force outweighs the viscous force of the fluid [21] and considering that the number of steps in the spillway in this research is the same for all models, the Reynolds number and the number of steps can be ignored.

2.3. Geometric model

Simulation has been carried out in order to investigate the performance of stepped spillways with reverse step barriers in terms of energy dissipation, by choosing five different configurations and comparing the results with the conventional step shape. In this study, the term reverse step barriers refers to physical barrier elements installed on the steps of the spillway. These barriers are additional structural components and should not be interpreted as modifications to the step geometry or orientation. Here, in the first stage of the simulation, the ratio of the flow velocity to the critical velocity (V/V_c) and also the critical depth to the step height (y_c/h) for a stepped spillway with a conventional step has been compared with the laboratory results [8] and the results of the numerical model, validated. The experiments were carried out using a stepped spillway, measuring 0.52 meters in width, consisting of 10 steps in a conventional shape. Step of the spillway measures 0.1 meters in height and 0.2 meters in width. The stepped spillway investigated by Felder et al. [8] is schematically illustrated in Figure 1. All the models investigated in this research have been drawn and meshed by Gambit software and then transferred to OpenFOAM software.

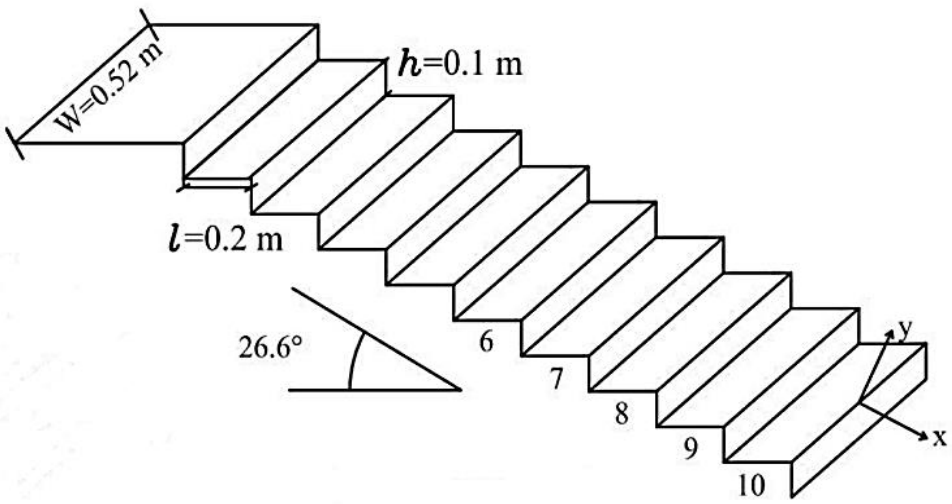


Fig. 1- Geometric configuration of the stepped spillway examined experimentally by Felder et al. [8].

2.4. OpenFOAM

OpenFOAM is a well-established open-source computational fluid dynamics (CFD) software package that is extensively used for a wide range of fluid-flow simulations. It is implemented in C++, a high-level, object-oriented programming language, making use of C++ programming language for all its codes, solvers, and libraries. In addition to the model and mesh generation tool, OpenFOAM can import the meshed model with defined boundary conditions file from various mesh generation software like Gambit and Netgen. OpenFOAM software offers a distinct advantage over commercial software like Fluent or Ansys when it comes to defining system parameters and selecting an appropriate solver based on the specific conditions of the problem. Various numerical methods, including finite volume, finite element, boundary element, and finite difference methods, can be employed to solve the governing equations of two-phase flow and determine unknown values. The process of solving these equations involves discretization and defining a system of equations within specific intervals of the solution domain for the unknown variables.

In the present study, numerical simulations were performed using the interFoam solver within the OpenFOAM framework. The InterFoam solver employs the Volume of Fluid (VOF) approach to simulate incompressible two-phase flows with a free surface. Rather than solving separate momentum equations for each phase, the method solves a single momentum equation for the mixture, with density and viscosity determined from the corresponding phase volume fractions. To track the air–water interface, the transport equation for the liquid-phase volume fraction is solved as follows:

$$\frac{\partial \alpha}{\partial t} + \nabla \cdot (\alpha U) + \nabla \cdot [\alpha(1-\alpha)U_r] = 0 \qquad (5)$$

where α is the volume fraction of the liquid phase, U is the mixture velocity, and Ur is the artificial relative velocity used for interface compression. The continuity equation for the mixture can be expressed as follows:

$$\nabla \cdot U = 0 \qquad (6)$$

The momentum equation for the two-phase mixture is expressed as follows:

$$\frac{\partial(\rho U)}{\partial t} + \nabla \cdot (\rho U U) = -\nabla p_{rgh} + \nabla \cdot \left[\mu_{eff}(\nabla U + \nabla U^T)\right] + \rho_g + f_\sigma \qquad (7)$$

where $\rho=\alpha\rho_1+(1-\alpha)\rho_2$ is the mixture density, μ_{eff} is the effective viscosity, p_{rgh} is the modified hydrostatic pressure, g is the gravitational acceleration, and fσ represents the surface tension force modeled using the Continuum Surface Force (CSF) approach.

To account for the nonlinear Reynolds stress term, it is necessary to incorporate a turbulence model. In this research, the RNG K-ε turbulence model has been employed for simulation. Although LES and the standard RNG k–ε turbulence models could also be employed in this study, the RNG k–ε model was selected owing to its capability to simulate flow through complex meshes, its use of fewer empirical constants in the governing relations, and its satisfactory performance in predicting flow separation regions. Also, the high capability of the $RNG\ K-\varepsilon$ turbulence model to simulate the flow over the stepped spillway and the vertical drop in the studies conducted by Rezapour and Tavakoli [22], Daneshfaraz and Ghaderi [23] and Ghaderi et al. [24] has been concluded. The research conducted in this study explored five three-dimensional configurations, as depicted in Figure 2. All 3D models include various step configurations with reverse step barriers. In

Figure 3, two types of barriers are selected and different arrangements of these barriers are used in stepped spillway configurations.

2.5. Meshing and boundary conditions

In this research, four different designs were employed to determine the suitable mesh size and ensure accurate correspondence between the flow velocity results obtained from both the numerical and laboratory models in step number 9. Ultimately, after careful evaluation, design number 2 was determined to be the optimal choice, featuring a total of 430,000 meshes. Table 2 displays the error parameters associated with the utilization of varying mesh quantities in the numerical results. Considering that in scenario 1 with an increase of 80,000 meshes compared to scenario 2, there was no significant change in the accuracy of the numerical results, in order to prevent the increase in computational cost, scenario 2 was selected as the superior design.

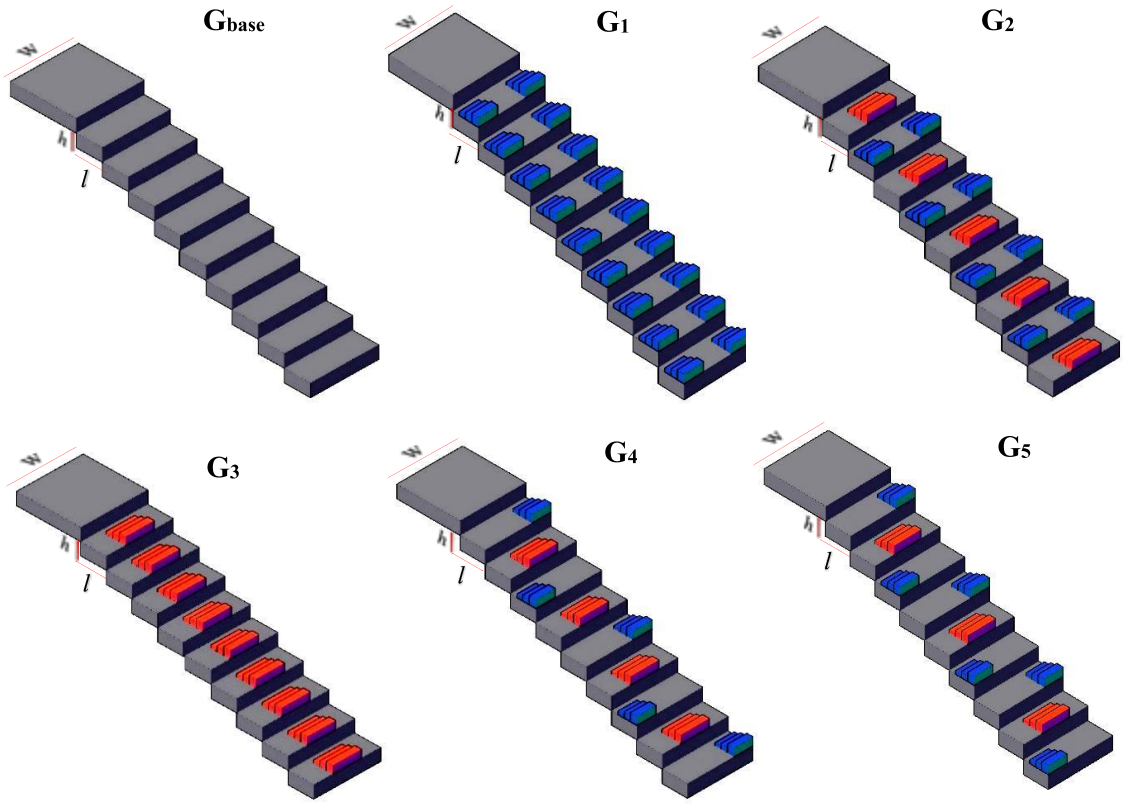


Fig. 2- Different arrangements of reverse step barriers in stepped spillway (W=52cm, h=10 cm and l=20cm)

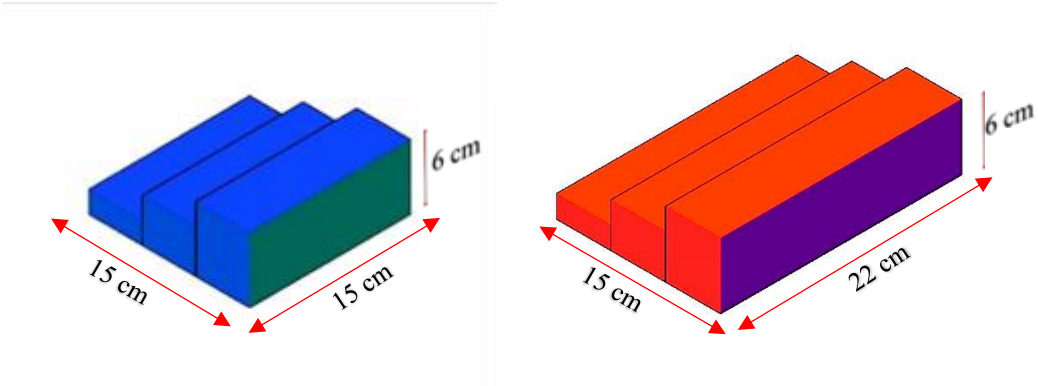


Fig. 3- Dimensions of reverse step barriers in different layouts

Table 2: Error parameters for the number of meshes used

Scenario	Mesh size (m)	Mesh Number	MAPE (%) $M = \frac{1}{n}\sum_{t=1}^{n}\left\|\frac{A_t - F_t}{A_t}\right\|$
1	0.008	510000	4.0
2	0.01	430000	4.2
3	0.03	360000	9.5
4	0.04	220000	15.1

In Table 2, MAPE means the mean absolute percentage error, A_t represents real laboratory values and F_t represents simulated numerical values. Finally, Figure 4 shows the boundary conditions and computational grid used in the models of this research.

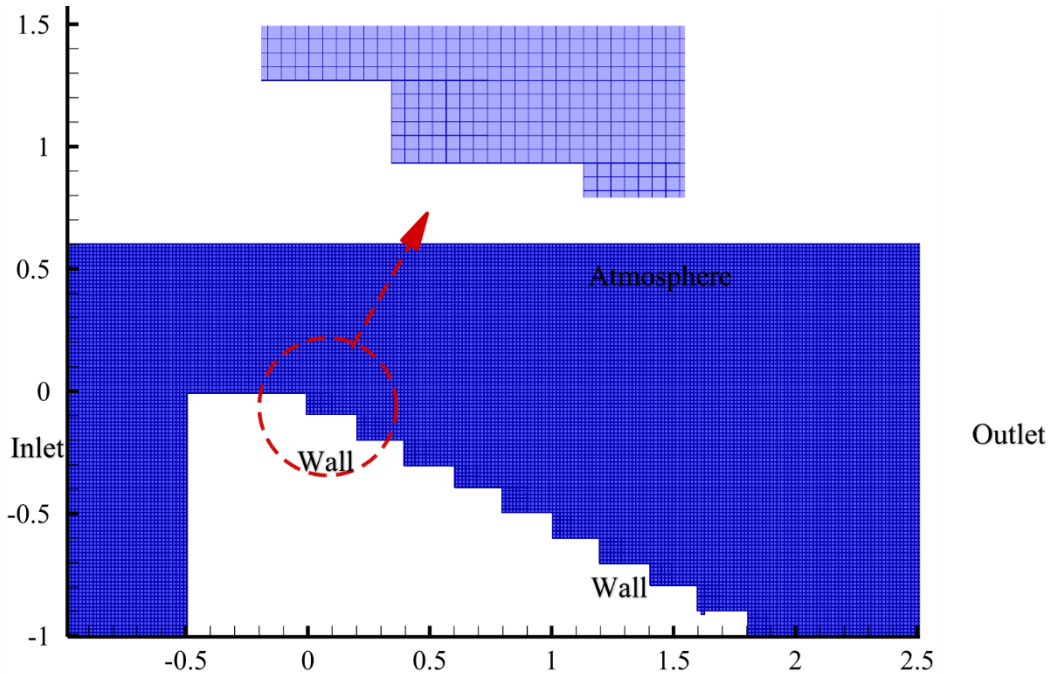


Fig. 4- Mesh configuration and boundary conditions used in the numerical model.

Boundary conditions were done separately for all parameters in OpenFOAM software. In this study, a mass-flow-rate boundary condition was specified at the inlet, while a pressure-outlet condition was imposed at the downstream boundary. The free surface was treated as an atmospheric boundary, and wall conditions were assigned to the spillway walls and bottom. A no-slip condition was applied to all solid surfaces, resulting in zero fluid velocity at the walls, while the flow field was resolved in the computational cells adjacent to the solid boundaries (near-wall cells).

3. Results and Discussion

3.1. Numerical Results Verification

To evaluate the numerical model's accuracy, a discharge of 0.09 m^3/s was selected, corresponding to the flow rate employed in the laboratory experiments of Felder et al. [8]. The simulated velocity distribution is presented in dimensionless form using $\left(\frac{V}{V_c}\right)$ and $\left(\frac{y}{y_c}\right)$, where y_c denotes the critical flow depth and (V_c) is the corresponding critical flow velocity. Figure 5 depicts the comparison between the velocity distributions of the numerical and experimental models for flat stepped spillways, specifically for a flow rate of 0.09 m^3/s. Upon examination of the findings, it is observed that the mean absolute percentage error (MAPE) for steps 7, 8, and 9 between the numerical and experimental results is determined to be 4.30%, 4.87%, and 4.20%, respectively. This shows that there is a good agreement between the results of the numerical model and the experimental data.

It should be noted that the velocity profiles shown in Figure 5 were extracted from sampling locations slightly above the step surface rather than directly at the wall. The first sampling locations are approximately y/y_c=0.02, 0.015, and 0.01 for Steps 7, 8, and 9, respectively. Therefore, the zero velocity at the wall prescribed by the no-slip boundary condition is fully satisfied.

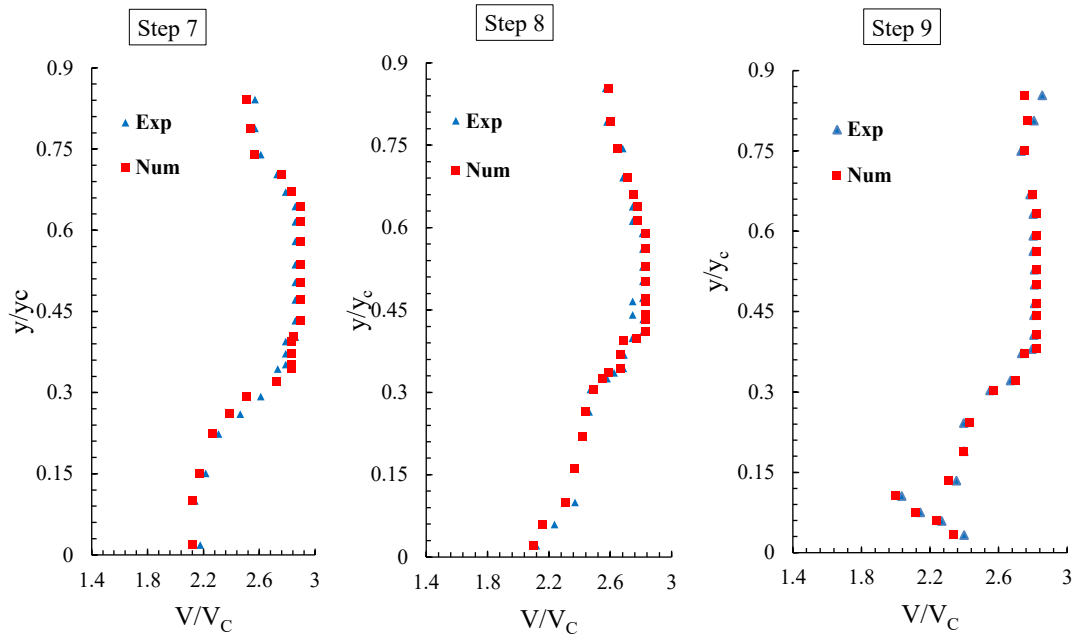


Fig. 5- Vertical distribution of flow velocity for steps 7, 8 and 9 (Q= 0.09 m^3/s)

3.2. Flow pattern

Figure 6 illustrates the streamlines in various configurations of a stepped spillway featuring reverse step barriers, along with a comparison to the scenario without any barriers. As it can be seen from this figure, the reverse step barriers have caused turbulence and significant changes in the streamlines. In the flat stepped spillway in the skimming flow regime, the streamlines are parallel to each other and the rotational flows are regularly formed under the pseudo bottom, but in other configurations, according to the location of reverse step barriers, the streamlines have taken different and irregular shapes.

3.3. Free surface profile

Figure 7 presents the water surface profile along the stepped spillways under skimming flow conditions at a discharge of 0.09 m³/s. Evidently, in the skimming flow regime, the water smoothly flows over the steps in a continuous layer. In this scenario, the steps function as an obstruction, introducing roughness to the flow. As a result, the primary cause of energy dissipation in this flow regime stems from the rotational flows generated beneath the pseudo bottom. In Figure 8, the presence of rotational flows beneath the pseudo bottom is evident in the stepped spillway model where a reverse slope replaces steps number 6 to 8.

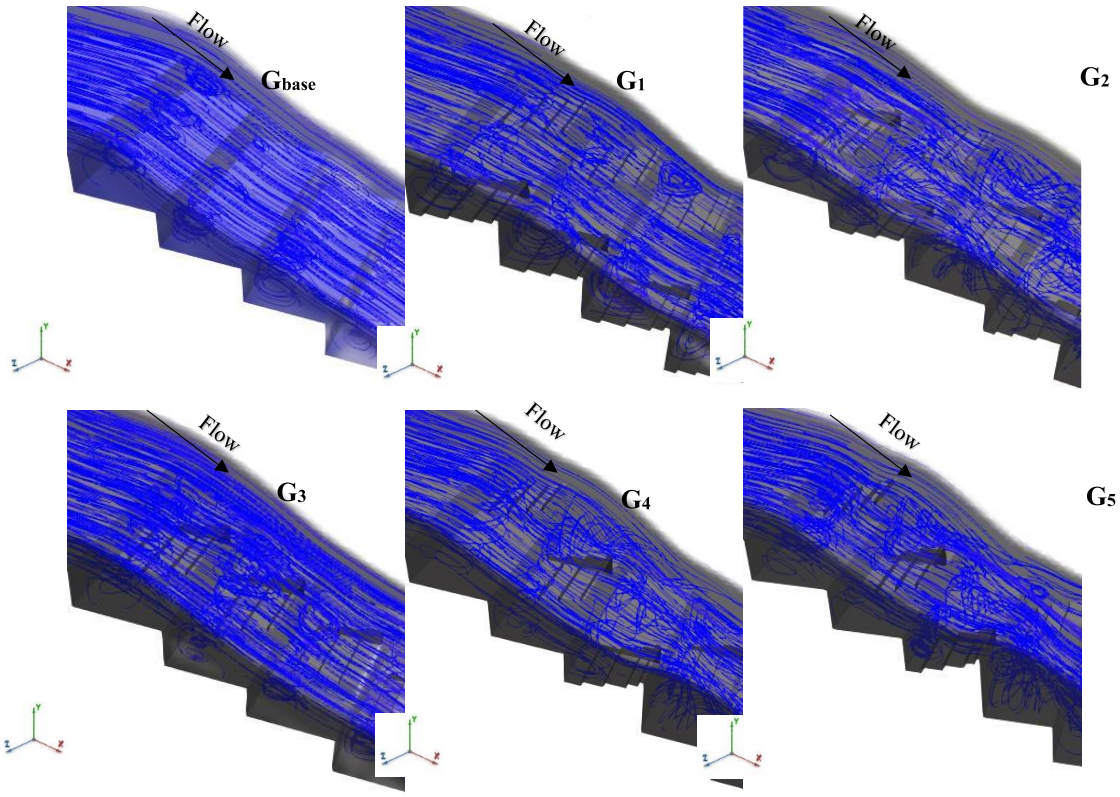


Fig. 6- The streamlines simulated on the stepped spillway, specifically with the flat step form (G_{base}) and various forms of reverse step barriers (G1-G5)

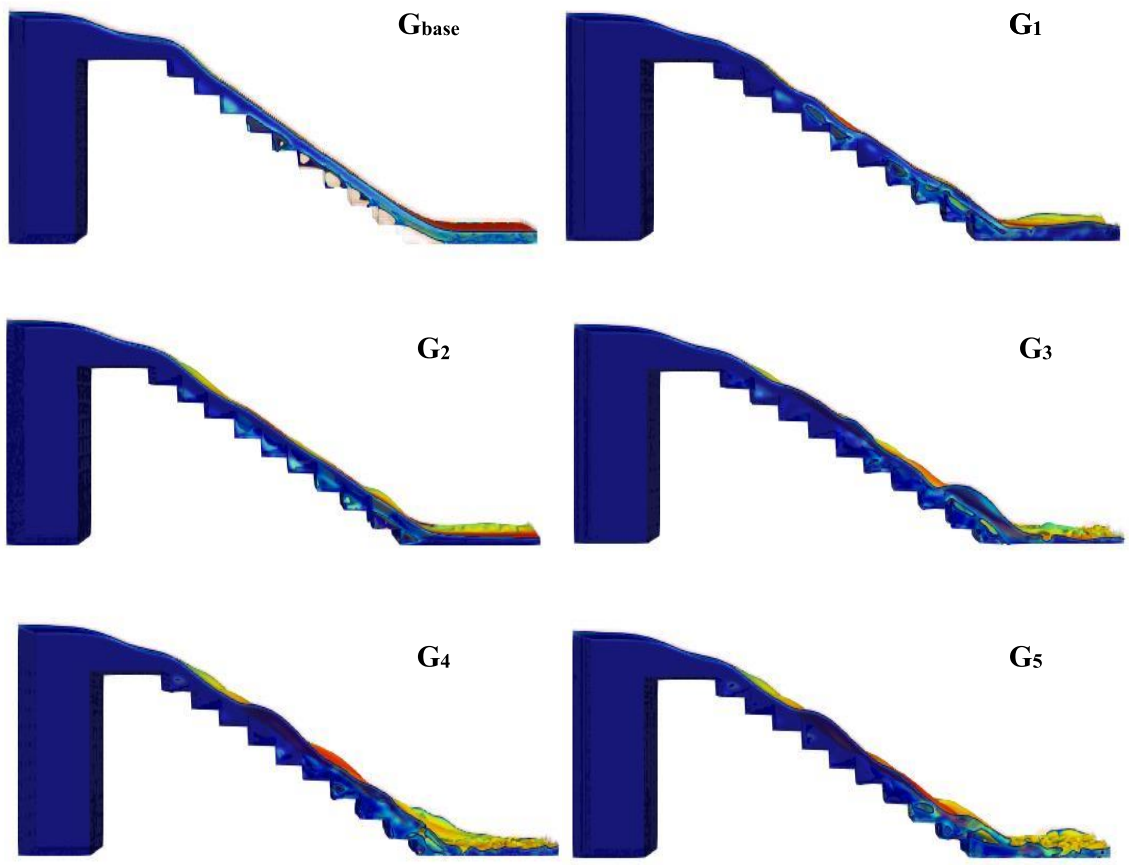


Fig. 7- Simulated free-surface profiles under skimming flow conditions for the stepped spillway with a flat-step configuration (G_{base}) and various reverse-step barrier configurations (G_1–G_5).

Based on the research results of Chanson [1], flow resistance is determined by the recirculation process resulting from rotating vortices in the recirculation area. Additionally, energy dissipation occurs due to the transfer of momentum between the flow in the cavity area and the main flow. The larger the recirculation area, the more flow energy dissipation will occur. Figure 8 shows the flow velocity over the stepped spillway models of this research.

The impact of these reverse step barriers is evident in the reduction of flow velocity from upstream to downstream. Consequently, the velocity reduction in the stepped spillway with reverse step barriers is significantly more pronounced in comparison to the conventional stepped spillway. As an illustration, the average velocity downstream of the end step in stepped spillways with reverse step slopes ranging from G2 to G5 has experienced respective decreases of 54.1%, 12.9%, 33.7%, and 38.6% when compared to the conventional stepped spillway. The decrease in flow velocity can be attributed to the interference of streamlines and the heightened resistance to flow caused by the presence of reverse step barriers.

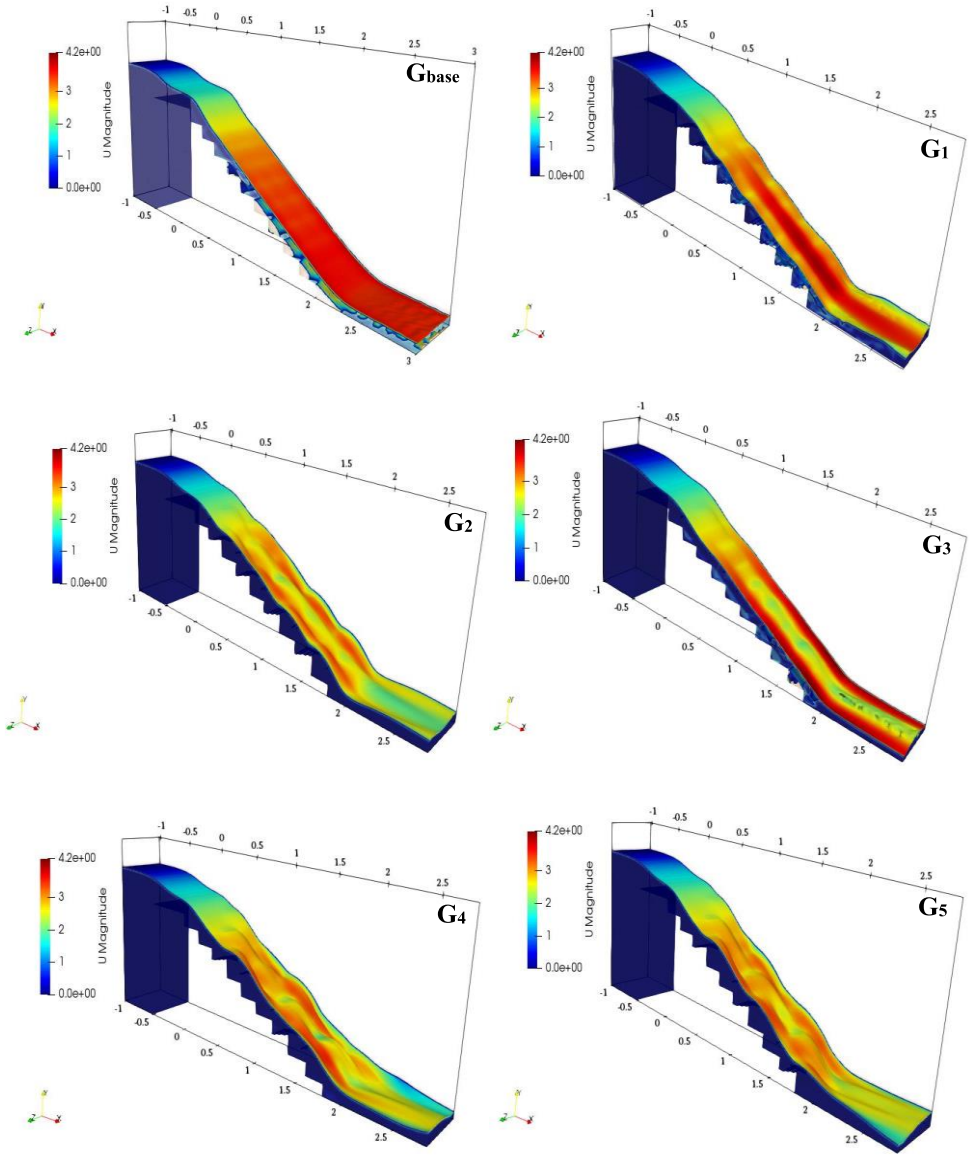


Fig. 8- Velocity distribution for stepped spillways with different reverse-step barrier configurations

3.4. Energy dissipation and residual energy

The transfer of water through spillways to the downstream inevitably results in a significant amount of kinetic energy. The presence of steps in stepped spillways leads to the dissipation of energy within the flow. The consideration of enhancing the impact of these steps on the level of energy dissipation has always been a subject of interest. One of the key concerns for hydraulic structure designers is determining the extent of energy dissipation in stepped spillways and the residual energy remaining at the end of this type of spillway. In this study, by making changes in the stepped spillway geometry and using reverse step barriers, the amount of energy dissipation was calculated in two forms $\left(\frac{\Delta H}{H_0}\right)$ and $\left(\frac{\Delta H}{H_{max}}\right)$ at the edge of the last step. The calculation of energy dissipation (η%) at each step of the stepped spillway is given as follows:

$$\eta\% = \frac{\Delta H}{H_0} = \frac{H_0 - H}{H_0}; \Delta H = H_0 - H \qquad (8)$$

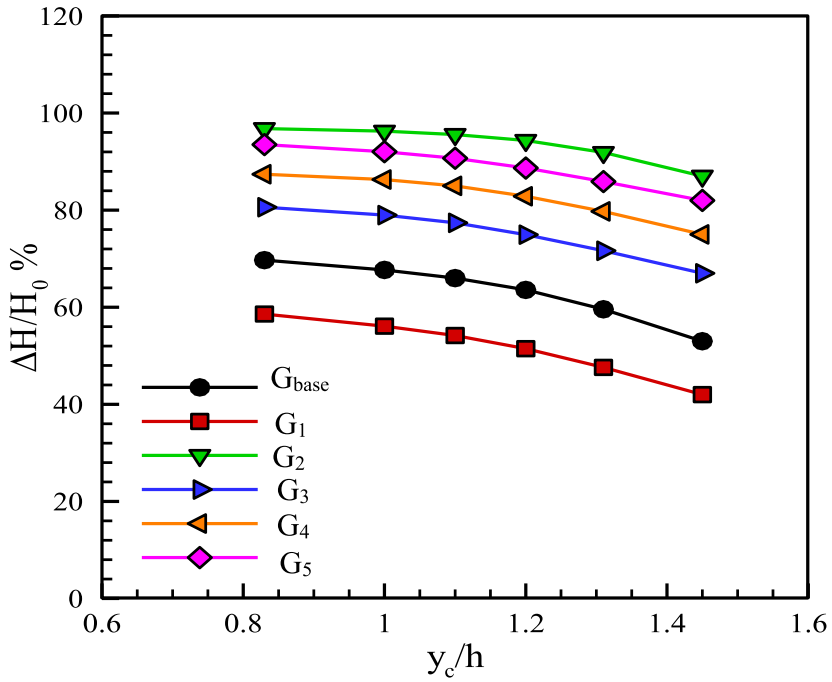


Fig. 9- Relative energy dissipation for different reverse-step barrier configurations compared with the flat stepped spillway

Figure 9 shows that the reverse step barriers configuration of the stepped spillway generally results in higher energy dissipation at the downstream end (final step). On the other hand, in the configuration of G_1, the dissipation rate has decreased compared to the basic plan. This is due to its distinctive configuration, which forms a pathway along the spillway's central axis, directing side flows toward the center, increasing flow velocities along the spillway path, and ultimately reducing energy dissipation relative to the base model. Among all the configurations, the configuration with G_2 geometry has the highest amount of energy dissipation. For a flow rate of 0.09 m^3/s and y_c/h =1.45, the stepped spillways with reverse step barriers G_2 to G_5 demonstrated 64.1%, 26.4%, 41.5%, and 54.7% higher energy dissipation compared to a conventional stepped spillway in the same flow conditions. Figure 10 shows the flow energy dissipation rate $(\frac{\Delta H}{H_{max}})$ in terms of dimensionless number $(\frac{\Delta z_0}{y_c})$ for all models. ΔZ_0 represents the vertical measurement from the spillway crest to the final step for all spillway models. Also, equation 9 can be used to calculate the maximum water height upstream of the spillway:

$$H_{max} = 1.5y_c + H_{spillway} \quad (9)$$

where $H_{spillway}$ is the spillway height and y_c is the critical depth. Also, to get the energy loss, it is necessary to calculate H_{res}, as follows:

$$H_{res} = dcos\theta + \frac{U_w^2}{2g} \quad (10)$$

In above equation, U_w, θ, d, and g are the flow velocity in the spillway central axis, the slope of the chute, the depth of the flow, and the acceleration of gravity, respectively.

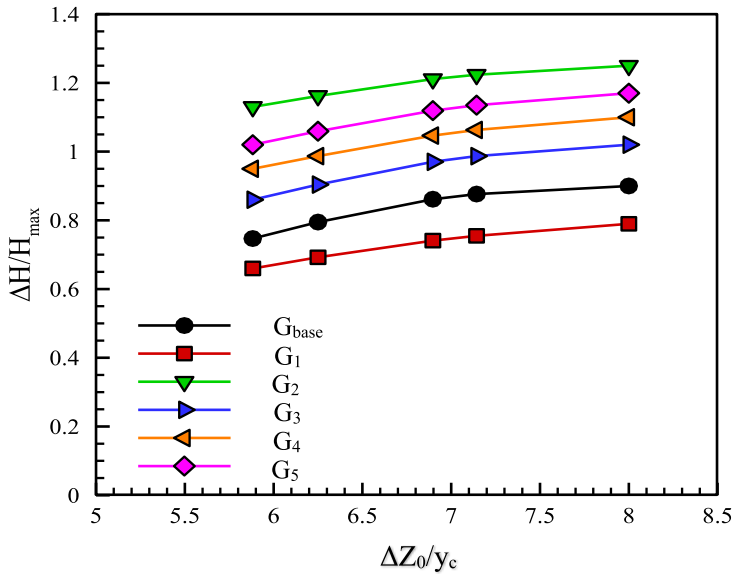


Fig. 10- Energy dissipation rate in different geometries: conventional stepped spillway (G_{base}) and different forms of reverse step barriers (G_1-G_5)

Figure 10 indicates that the energy dissipation rate in all of the stepped spillways with reverse step barriers, except for G_1 geometry, was higher than the flat stepped spillway. The reason for this is the roughness caused by the steps in designs with reverse step barriers in the flow path. As a result, due to the high interference of streamlines, creating more disturbances in the spillway path, more flow energy dissipation has been achieved. According to Figure 10, G_2 geometry has created the highest energy dissipation rate. Therefore, this configuration is proposed as a desirable option to dissipate as much flow energy as possible in stepped spillways. Figure 11 illustrates the relationship between the dimensionless residual height (H_{res}/y_c) and the dimensionless ratio of critical depth to step height (y_c/h).

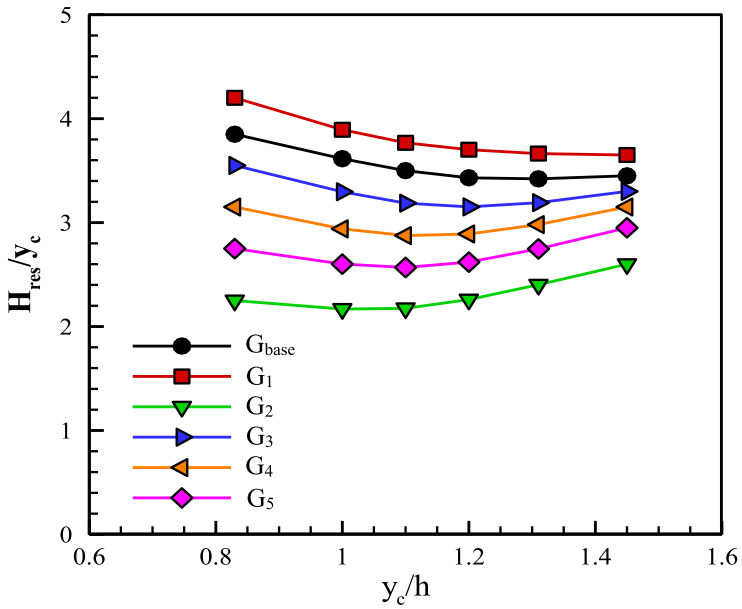


Fig. 11- Residual energy in different geometries of stepped overflow with flat form (G_{base}) and different forms of reverse step barriers (G_1-G_5)

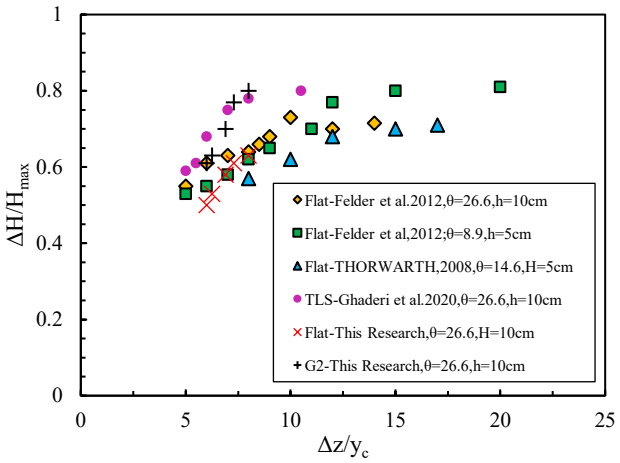


Fig 12 - Comparison of energy dissipation rates between the present model and those reported in previous studies

Under identical flow conditions, the flat stepped spillway exhibits a higher residual energy level than the reverse-step configuration G2. For example, at $y_c/h=1.45$, the dimensionless residual head for the flat stepped spillway reaches $H_{res}/y_c = 3.49$, whereas for stepped spillway with the G2 form it equals $H_{res}/y_c = 2.6$. To validate the numerical model, the simulation results obtained for the conventional stepped spillway were comprehensively compared with the well-established experimental data reported by Felder *et al.* [8] and Thorwarth [25]. The comparison demonstrated a satisfactory quantitative and qualitative agreement between the numerical predictions of the present study and the corresponding experimental observations. Furthermore, the energy dissipation performance of the G2 stepped spillway configuration was evaluated against the numerical results reported by Ghaderi *et al.* [26]. Despite variations in the boundary conditions and geometric arrangements of the models, the results indicate that the variation trend of the energy dissipation rate obtained in the present study is in good agreement with the behavioral patterns reported in the reference studies. The consistency observed across the investigated scenarios (Fig. 12) further confirms the accuracy of the numerical approach and demonstrates the reliability and predictive capability of the present model for analyzing the complex hydraulic processes governing energy dissipation in stepped spillways. Consequently, the proposed numerical model provides a reliable basis for engineering-scale investigations of stepped spillway hydraulic performance.

4. Conclusions

For many years, stepped spillways have been employed as a means to effectively manage the destructive force of flow on spillways, resulting in reduced dimensions of stilling basins and associated costs. Over time, researchers have presented numerous designs and configurations aimed at enhancing the performance of these spillways. In this study, the researchers aimed to introduce a novel design for stepped spillways known as stepped spillway with reverse step barriers. The hydraulic performance of this configuration was then examined using OpenFOAM software in three dimensions, with the goal of enhancing energy dissipation conditions. According to the research, the following results were obtained:

- The velocity distribution results obtained from comparing the experimental data of

Felder et al. [11] with the results from OpenFOAM software showed a maximum error of 4.87% at step number 8. This indicates a satisfactory level of agreement between the laboratory data and the numerical results.

- Due to the greater roughness caused by the reverse step barriers, the rate of flow interference has increased along the path, and in addition to the rotational flows created in different sections, the rate of interference and subsequently energy dissipation has increased.
- The reverse step barrier has reduced the flow velocity when moving to the downstream of the spillway. In the basin downstream of the final step, the average velocity values were recorded. The findings showed that, relative to the conventional stepped spillway, the flow velocity in stepped spillways G2 to G5 decreased by 54.1%, 12.9%, 33.7%, and 38.6%, respectively. The decrease in flow velocity can be attributed to the interference of streamlines and the increase in flow resistance caused by the presence of reverse step barriers.
- The incorporation of reverse-step barriers into the stepped spillway enhances energy dissipation, with the most pronounced effects occurring near the downstream end of the spillway and on the final step. Also, among different configurations of stepped overflow with reverse step barriers, G_2 geometry has obtained the highest dissipation rate. For a flow rate of 0.09 m^3/s and $y_c/h=1.45$, the stepped spillways with reverse step barriers (G_2 to G_5) exhibit 64.1%, 26.4%, 41.5%, and 54.7% higher energy dissipation compared to a conventional stepped spillway under identical flow conditions.
- Under the same flow conditions, the G2 configuration produces a lower residual energy level than the conventional stepped spillway, indicating its greater effectiveness in energy dissipation. When $y_c/h=1.45$, the value of dimensionless residual height for a flat stepped spillway is equal to $H_{res}/y_c=3.49$, while the value of this parameter for the stepped spillway of the reverse step barriers with G_2 form is equal to $H_{res}/y_c=2.6$.
- Based on the current research, G_2 geometry was suggested as the best-performing configuration in stepped spillways with reverse step barriers in terms of energy dissipation rate.

Conflicts of interest

The authors declare that they have no known competing financial interests or personal relationships that could have appeared to influence the work reported in this paper.

Funding

This research did not receive any specific grant from funding agencies in the public, commercial, or not-for-profit sectors.

References

1. Chanson H. (1994). State of the art of the hydraulic design of stepped chute spillways. Hydropower Dams, 1(4), 33–42.
2. Sorensen, R. M. (1985). Stepped spillway hydraulic model investigation. Journal of Hydraulic Engineering, 111(12), 1461–1472.
3. Peyras, L., Royet, P., & Degoutte, G. (1992). Flow and energy dissipation over stepped gabion weirs. Journal of Hydraulic Engineering, 118(5), 707–717.
4. Rice, C. E., Robinson, K. M., & Kadavy, K. C. (1996). Rock riprap for grade control. Proceedings of the North American Water and Environment Congress.
5. Chanson H. The hydraulics of stepped chutes and spillways. A.A. Balkema, Lisse, The Netherlands, pp. 1-14. Balkema; 2002.
6. Felder, S., & Chanson, H. (2009). Turbulence, dynamic similarity and scale effects in high-velocity free-surface flows

above a stepped chute. Experiments in Fluids, 47(1), 1–18.
7. Felder, S., Fromm, C., & Chanson, H. (2012). Air entrainment and energy dissipation on a 8.9° slope stepped spillway with flat and the steps. Hydraulic Model Report No. CH86/12, University of Queensland.
8. Felder, S., Guenther, P., & Chanson, H. (2012). Air–water flow properties and energy dissipation on stepped spillways. Hydraulic Model Report No. CH87/12, University of Queensland.
9. Hamedi, A., Malekmohammadi, I., Mansoori, A., & Roshanaei, H. (2012). Energy dissipation in stepped spillway equipped with inclined steps together with end sill. Proceedings of the Fourth International Conference on Computational Intelligence and Communication Networks.
10. Nohani, E. (2014). An experimental study on the effect of vortex breakers on discharge coefficient for shaft spillways. Journal of Civil Engineering and Urbanism, 4(5), 546–549.
11. Li, S., & Zhang, J. (2018). Numerical investigation on the hydraulic properties of the skimming flow over pooled stepped spillways. Water, 10(10), 1478.
12. Ma, X., Zhang, J., & Hu, Y. (2022). Analysis of energy dissipation of interval-pooled stepped spillways. Entropy, 24(1), 85.
13. Salmasi, F., & Abraham, J. (2022). Genetic algorithms for optimizing stepped spillways to maximize energy dissipation, Water Supply, IWA Publishing, 22(2), 1255.
14. Salmasi, F., & Abraham, J. (2022). Effect of slope on energy dissipation for flow over a stepped spillway,
15. Water Supply, 22(5), 5056-
16. Salmasi, F., & Abraham, J. (2023). Hydraulic characteristics of flow over stepped and chute spillways (case tudy: Zirdan Dam), Water Supply, 23(2), 851-866.
17. Salmasi, F., Razi, S., & Abraham, J. (2023). Hydraulics of flow in gabion stepped spillways, an experimental study, Journal of Hydraulic Structures, 2023; 9(2):75-100.
18. Ghaderi, D., Ebrahimnezhadian, H., & Mollazadeh, M. (2023). A three-dimensional study of flow characteristics over different forms of stepped–labyrinth spillways in the skimming flow regime. AQUA-Water Infrastructure, Ecosystems and Society, 72(8), 1415-1430.
19. Ghaderi, D., Ebrahimnezhadian, H., & Mollazadeh, M. (2024). Three-dimensional analysis of the performance of circular stepped spillways in the skimming flow regime, Journal of the Brazilian Society of Mechanical Sciences and Engineering, 46, 415
20. Rajaratnam, N. (1990). Skimming flow in stepped spillways. Journal of Hydraulic Engineering, 116(4), 587–591.
21. Chanson H. (2000). Historical development of stepped cascades for the dissipation of hydraulic energy. Trans Newcomen Soc., 72(2), 295–318.
22. Chow VT. Open-channel hydraulics. McGraw-Hill; 1959.
23. Rezapour Tabari, M., & Tavakoli, S. (2016). Effects of stepped spillway geometry on flow pattern and energy dissipation. Arabian Journal for Science and Engineering, 41(4), 1215–1224.
24. Daneshfaraz, R., & Ghaderi, A. (2017). Numerical investigation of inverse curvature ogee spillway. Civil Engineering Journal, 3(11), 1146–1156.
25. Ghaderi, A., Dasineh, M., & Abbasi, S. (2019). Impact of vertically constricted entrance on hydraulic characteristics of vertical drop. Journal of Hydraulics, 13(4), 121–131.
26. Thorwarth, J. (2008). Hydraulics of pooled stepped spillways- self-induced unsteady flow and energy dissipation. Ph.D. Thesis, University of Aachen, Aachen, Germany.
27. Ghaderi, A., Daneshfaraz, R., Dasineh, M. & Di Francesco, S. (2020). Energy Dissipation and Hydraulics of Flow over Trapezoidal-Triangular Labyrinth Weirs. Water 12, 1992.

© 2026 by the authors. Licensee SCU, Ahvaz, Iran. This article is an open access article distributed under the terms and conditions of the Creative Commons Attribution 4.0 International (CC BY 4.0 license) (http://creativecommons.org/licenses/by/4.0/).